23rd ABCM International Congress of Mechanical Engineering
December 6-11, 2015, Rio de Janeiro, RJ, Brazil

ANALYSIS OF A HIGH ORDER LES CODE FOR TURBULENT BOUNDARY LAYER SIMULATION

Patrícia Sartori
Leandro Franco de Souza
Department of Applied Mathematics and Statistics, ICMC - University of Sao Paulo, Sao Carlos, Sao Paulo, Brazil
psartori26@gmail.com, lefraso@gmail.com

Abstract. *The success of turbulent boundary layer simulation is especially associated with the precise prescription of inflow information. Random Flow Generation (RFG) technique is based on scaling and orthogonal transformation operations applied to a continuous flow-field generated as a superposition of harmonic functions and allows to generate non-homogeneous anisotropic flow field representing turbulent velocity fluctuations. In this sense, this study investigates the ability of a high order LES code in combination with RFG technique for simulating high-Reynolds number flows in a zero pressure gradient flat plate. The results of velocity means and Reynolds stress averages show a good match to DNS and LES data from the literature.*

Keywords: *turbulent boundary layer, inflow modelling, LES simulations*

1. INTRODUCTION

The numerical study of turbulence is still a major challenge in CFD area due to its inherently three-dimensional and time-dependent behaviour. For years many efforts have been made on the development of numerical tools for the simulation of turbulent flows. The main methodologies used to study numerically turbulent flows are DNS (Direct Numerical Simulation), RANS (Reynolds Averaged Navier-Stokes) and LES (Large Eddy Simulation).

DNS captures all scales of the turbulent flow then it requires a extremely refined grid and time step. Then, in the most of cases this methodology exceeds the capacity of the most powerful computers currently available (Lesieur and Métais, 1996).

In RANS the dependent variables are decomposed into mean and fluctuating parts by applying time average in Navier-Stokes equations. As results, only the averaged motion is computed and the effect of fluctuations is modelled. The advantage is the lower computational cost. However, this methodology does not capture detailed information of the flow, since these are lost by applying the time average.

In the LES approach, the turbulent scales are split into two groups: the group of large scales and small scales. The large scales are resolved directly, while small scales are modelled using so-called sub-grid scale models (Wilcox, 1994; Lesieur and Métais, 1996). Due to the separation process, LES has become an alternative with a smaller computational effort than DNS simulations, then it can be applied to solve flows with higher Reynolds numbers justifying its growth use in recent years.

A factor influencing in the success of LES simulations is the appropriate choice of the initial conditions for the problem. In fact, it is a highly dependent phenomenon of imposed boundary conditions where small perturbations in these conditions result in getting erroneous magnitude to the physical properties of the flow.

In this paper, the objective is to investigate a 3D high order LES code using the efficient Random Flow Generation (RFG) technique (Smirnov *et al.*, 2001) to introduce realistic inflow conditions for simulating turbulent flows in a zero pressure gradient flat plate. The RFG method can be used to prescribe inlet conditions as well as initial conditions for spatially developing inhomogeneous and anisotropic turbulent flows. For the sub-grid modelling is adopted the WALE model.

2. MATHEMATICAL FORMULATION

This section presents the theoretical framework and the governing equations for Large Eddy Simulation of incompressible turbulent flows. The vorticity-velocity formulation is taken as an alternative to the primitive equations.

2.1 LES - Large Eddy Simulation

Understanding turbulence phenomena is one of the most intriguing and challenging problems of all classical physics and has been subject of study for many centuries (Pope, 2000). In fact, the high degree of freedom combined with its random behaviour make this a very difficult task. As mentioned earlier, the DNS simulations of turbulent flows are limited to simple geometries at low Reynolds numbers due to high computational cost for solving all scales of turbulence.

The fundamental principle of the LES methodology is the separation of large and small scales of turbulence through a spatial filtering process (Lesieur and Métais, 1996; Sagaut, 2006). The filtering process is applied on primitive governing equations and the separation of scales is controlled by a characteristic filter width (Δ_c), where Δ_c determines the cutoff frequency. Then, the scales that have a greater size than the cutoff frequency are called a large scale (filtered) while the other ones are called small scales (sub-grid scales) (Lesieur and Métais, 1996; Sagaut, 2006). As result, the filtered variables are resolved directly from the filtered equations and the smaller structures are modelled. After the separation process an additional tensor appears and it is replaced by a sub-grid scale model that introduces the effect of small scales on the filtered equations (Germano *et al.*, 1991).

2.2 LES equations

The flow is governed by the filtered, unsteady, three-dimensional incompressible Navier-Stokes and continuity equations:

$$\frac{\partial u_i}{\partial t}+\frac{\partial (u_i u_j)}{\partial x_j} = -\frac{1}{\rho_0}\frac{\partial P}{\partial x_i}+\frac{\partial}{\partial x_j}\left[\nu\left(\frac{\partial u_i}{\partial x_j}+\frac{\partial u_j}{\partial x_i}\right)+\tau_{ij}\right], \tag{1}$$

$$\frac{\partial u_i}{\partial x_i} = 0, \tag{2}$$

where u_i, $i=1,3$ are the velocity vector components in the x_i coordinate direction, and P is the pressure. ρ_0 and ν are the density and kinematic viscosity of the fluid, respectively. The variable t denotes the time. The sub-grid scale tensor τ_{ij} results from the unresolved sub-grid scale and must be modelled by a sub-grid scale model.

Assuming $\tau_{ij} = 2\nu_t S_{ij} + \frac{1}{3}\tau_{kk}\delta_{ij}$ (Boussinesq's hypothesis), one gets

$$\frac{\partial u_i}{\partial t}+\frac{\partial (u_j u_i)}{\partial x_j} = -\frac{1}{\rho_0}\frac{\partial P_m}{\partial x_i}+2\frac{\partial}{\partial x_j}[(\nu+\nu_t)S_{ij}], \tag{3}$$

where $P_m = P - \frac{1}{3}\rho_0\tau_{kk}$ is a modified pressure. δ_{ij} is Kronecker delta and ν_t is sub-grid scale eddy viscosity. The deformation tensor of the filtered field is defined as $S_{ij} = \frac{1}{2}\left(\frac{\partial u_i}{\partial x_j}+\frac{\partial u_j}{\partial x_i}\right)$.

After the non-dimensionalization, the filtered Navier-Stokes and continuity equations can be rearranged as

$$\frac{\partial u_i^*}{\partial t^*}+\frac{\partial (u_j^* u_i^*)}{\partial x_j^*} = -\frac{\partial P_m^*}{\partial x_i^*}+\frac{1}{Re}\nabla^2 u_i^* + F_{\nu x_i}, \qquad \text{with} \qquad F_{\nu x_i} = \nu_t^*\nabla^2 u_i^* \tag{4}$$

$$\frac{\partial u_i^*}{\partial x_i^*} = 0, \tag{5}$$

where the non-dimensional variables $(*)$ can be written as

$$t=\frac{t^* L}{U_\infty}, \quad x_j = x_j^* L, \quad u_j = u_j^* U_\infty, \quad P=\rho_0 U_\infty^2 P_m^*, \quad \nu_t = L U_\infty \nu_t^*, \quad \tau_{kk} = \frac{\nu U_\infty}{L}\tau_{kk}^*, \quad P_m^* = P^* - \frac{1}{3Re}\tau_{kk}^*. \tag{6}$$

The Reynolds number is defined as $Re = \frac{U_\infty L}{\nu}$, where L is characteristic plate length and U_∞ is the reference velocity. ∇^2 denotes the Laplacian operator. In the next equations, the symbol $(*)$ will be omitted to facilitate the symbolism.

Now, the question is how ν_t should be modelled in order to better estimate the effects of sub-grid scales in the filtered solution. In this paper, the WALE (*Wall-Adapting Local Eddy-viscosity*) sub-grid scale model proposed by Nicoud and Ducros (1999) is adopted:

$$\nu_t = C_{\mathrm{W}}\Delta_c \frac{(S_{ij}^d S_{ij}^d)^{3/2}}{(S_{ij}S_{ij})^{5/2}+(S_{ij}^d S_{ij}^d)^{5/4}}, \tag{7}$$

where $C_{\mathrm{W}} = 0.104$ is a constant, $S_{ij}^d = \frac{1}{2}(g_{ij}^2+g_{ji}^2) - \frac{1}{3}\delta_{ij}g_{kk}^2$ and $g_{ij} = \frac{\partial u_i}{\partial x_j}$. One of the advantages of this model is that the eddy viscosity tends to zero near the wall, eliminating the use of damping functions.

2.3 Vorticity-velocity formulation

In this study, the vorticity-velocity formulation is used as an alternative of the primitive variables formulation in order to eliminate the pressure terms from filtered governing equations. Assuming the vorticity ω of a flow as $\omega = -\nabla \times \mathbf{u}$, the vorticity vector components become

$$\omega_x = \frac{\partial v}{\partial z}-\frac{\partial w}{\partial y}, \qquad \omega_y = \frac{\partial w}{\partial x}-\frac{\partial u}{\partial z}, \qquad \omega_z = \frac{\partial u}{\partial y}-\frac{\partial v}{\partial x}, \tag{8}$$

where u, v and w are the velocity vector components of vector **u** in the x, y and z directions, respectively.

Thus, the non-dimensional filtered Navier-Stokes equations (Eq. (4)) result in transport equations for the components of vorticity in x-, y-, and z- directions:

$$\frac{\partial \omega_x}{\partial t} + \frac{\partial a}{\partial y} - \frac{\partial b}{\partial z} = \frac{1}{Re}\nabla^2 \omega_x + \frac{\partial F_{\nu y}}{\partial z} - \frac{\partial F_{\nu z}}{\partial y}, \tag{9}$$

$$\frac{\partial \omega_y}{\partial t} + \frac{\partial c}{\partial z} - \frac{\partial a}{\partial x} = \frac{1}{Re}\nabla^2 \omega_y + \frac{\partial F_{\nu z}}{\partial x} - \frac{\partial F_{\nu x}}{\partial z}, \tag{10}$$

$$\frac{\partial \omega_z}{\partial t} + \frac{\partial b}{\partial x} - \frac{\partial c}{\partial y} = \frac{1}{Re}\nabla^2 \omega_z + \frac{\partial F_{\nu x}}{\partial y} - \frac{\partial F_{\nu y}}{\partial x}, \tag{11}$$

where $a = \omega_x v - \omega_y u$, $b = \omega_z u - \omega_x w$, and $c = \omega_y w - \omega_z v$ are the nonlinear terms. The Poisson equations for u, v and w are as follows:

$$\frac{\partial^2 u}{\partial x^2} + \frac{\partial^2 u}{\partial z^2} = -\frac{\partial \omega_y}{\partial z} - \frac{\partial^2 v}{\partial x \partial y}, \tag{12}$$

$$\frac{\partial^2 v}{\partial x^2} + \frac{\partial^2 v}{\partial y^2} + \frac{\partial^2 v}{\partial z^2} = -\frac{\partial \omega_z}{\partial x} + \frac{\partial \omega_x}{\partial z}, \tag{13}$$

$$\frac{\partial^2 w}{\partial x^2} + \frac{\partial^2 w}{\partial z^2} = \frac{\partial \omega_y}{\partial x} - \frac{\partial^2 v}{\partial y \partial z}. \tag{14}$$

2.4 Inflow modelling

The simulations of turbulent flows are heavily influenced by the choice of the inflow modelling technique. Due to the unsteady and pseudo-random characteristics of most real flows, the prescription of time-dependent turbulent inflow data is a challenge for numerical simulation approaches.

Many turbulent flow simulations begin from a quiescent flow or with the mean velocities obtained from RANS simulations. Unfortunately, this strategy takes a long time for the flow to develop spatially and temporally (Smirnov *et al.*, 2001). An alternative to solve this problem is to consider a separate flow solver with periodic boundary conditions to generate inlet conditions for LES/DNS simulations. However, its implementation can be not easy for well defined problems without fully developed boundary/shear layers and has a high computational cost for some engineering problems.

According to Keating *et al.* (2004) and Pamies *et al.* (2009), the methods found to overcome these situation are basically divided into two categories: *recycling methods* and *synthetic turbulence methods*. In the *recycling methods*, the turbulent flow is pre-calculated and re-introduced at the inlet of the computational domain (Lund, 1998; Li *et al.*, 2000). On the other hand, in the *synthetic turbulence methods* some random fluctuation is created and combined with the mean flow at the inflow. Most of the work done in this direction is based on simplified variants of the spectral method, in which Fourier harmonics are generated with the appropriate statistics and assembled into a random flow-field (Kraichnan, 1970; Smirnov *et al.*, 2001).

The synthetic Random Flow Generator (RFG) method proposed by Smirnov *et al.* (2001) was developed on the basis of the work of Kraichnan (1970), and can be used to prescribe inlet conditions as well as initial conditions for spatially developing inhomogeneous and anisotropic turbulent flows. It is based on Fourier decomposition, with Fourier coefficients computed from spectral data obtained at different locations across the turbulent flow based on the local team and length scales (Jarrin *et al.*, 2009). Also, it involves scaling and orthogonal transformation operations applied to a continuous flow-field generated as a superposition of harmonic functions. The RFG method is describe below:

1. Given an anisotropic velocity correlation tensor $r_{ij} \equiv \overline{\tilde{u}_i \tilde{u}_j}$, find an orthogonal transformation tensor a_{ij} that would diagonalize r_{ij}:

$$a_{mi} a_{nj} r_{ij} = \delta_{mn} c_{(n)}^2, \qquad a_{ik} a_{kj} = \delta_{ij}. \tag{15}$$

   As a result of this step both a_{ij} and $c_i = \{c_1, c_2, c_3\}$ become known functions of space.

2. Generate a transient flow-field $\{v_i(x_j, t)\}_{i,j=1,...3}$ in a 3D domain using the modified method of Kraichnan (Kraichnan, 1970):

$$v_i(\vec{x}, t) = \sqrt{\frac{2}{N}} \sum_{n=1}^{N} [p_i^n \cos(\tilde{k}_j^n \tilde{x}_j + \omega_n \tilde{t}) + q_i^n \sin(\tilde{k}_j^n \tilde{x}_j + \omega_n \tilde{t})], \tag{16}$$

$$\tilde{x}_j = \frac{x_j}{l}, \qquad \tilde{t} = \frac{t}{\tau}, \qquad c = \frac{l}{\tau}, \qquad \tilde{k}_j^n = k_j^n \frac{c}{c_{(j)}}, \tag{17}$$

$$p_i^n = \varepsilon_{i,j,m} \zeta_j^n k_m^n, \qquad q_i^n = \varepsilon_{i,j,m} \xi_j^n k_m^n, \quad \text{with} \quad \zeta_i^n, \xi_i^n, \omega_n \in N(0,1) \quad \text{and} \quad k_i^n \in N(0,1/2), \tag{18}$$

where l, τ are the length and time-scales of turbulence in the non-dimensional expressions. Coefficients $c_i, i = 1,2,3$ are the turbulent fluctuating velocities u_i' in the new coordinate system produced by the transformation tensor a_{ij}. $\varepsilon_{i,j,k}$ is the permutation tensor used in the vector product operation, and $N(M,\sigma)$ is a normal distribution with mean M and standard deviation σ. Numbers k_j^n, ω_n represent a sample of wave-number vectors and frequencies of the modelled turbulence spectrum:

$$E(k) = 16 \left(\frac{2}{\pi}\right)^{1/2} k^4 \exp(-2k^2). \tag{19}$$

3. Apply a scaling and orthogonal transformations to the flow-field v_i to obtain a new flow-field u_i:

$$w_i = c_{(i)} v_{(i)}, \qquad u_i = a_{ik} w_k. \tag{20}$$

The outcome of this procedure is a time-dependent flow-field $u_i(x,t)$ that is divergence free for a homogeneous turbulence and to a high-degree divergence-free for an inhomogeneous turbulence. Moreover, temporal and spatial correlations are guaranteed.

2.5 Boundary conditions

Figure 1 shows the computational domain where the equations Eq. (9) - (14) are solved. The boundary conditions used at the upper boundary is $\omega_x = \omega_y = \omega_z = 0$ (the flow is supposed to be irrotational). At the wall, the no-slip condition is assumed then u, v, and w are set zero. At the outflow boundary, second derivative of the velocity and vorticity components in the x-direction are set zero. At the inflow it is specified a boundary condition based on Blasius boundary layer solutions added to the fluctuations generated by the RFG method. In the region between x_1 and x_2, a buffer zone is adopted, where the fluctuations are damped in order to prevent numerical reflections at outflow boundary.

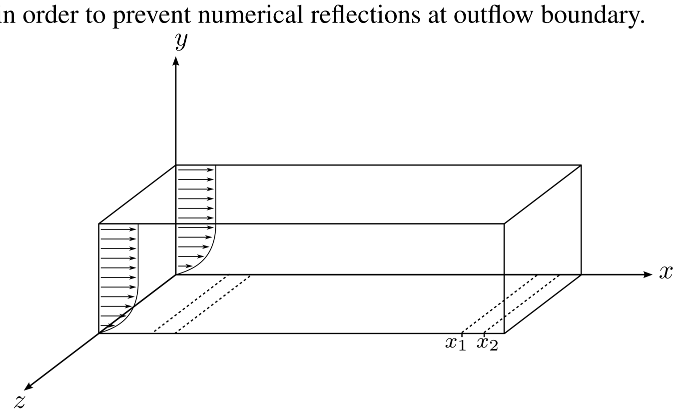

Figure 1. Computational domain

3. NUMERICAL FORMULATION

Streamwise and wall-normal derivatives are approximate using high order compact finite difference schemes. A 4^{th} order Runge-Kutta method is adopted for temporal integration of the transport of vorticity equations. The solution of V - Poisson equation is done via a multigrid method called Full Approximation Scheme. In order to reduce the computational cost and improve numerical resolution near to the wall, a technique known as grid stretching is implemented in the wall-normal direction. In the present paper, the stretching factor stf is constant then the spacing between the computational points in the wall-normal direction is obtained by a geometric progression. Moreover, the code is parallelized by domain decomposition strategy in the streamwise direction using the Message Passing Interface library for the communication among processors.

This paper assumes periodicity in z-direction therefore it is adopted a spectral method in this direction. Using the conditions of periodicity, all variables can be written as combinations of K Fourier modes

$$f(x,y,z,t) = \sum_{k=0}^{K} F_k(x,y,t) e^{-i\beta_k z}, \tag{21}$$

where f is a generic variable, $i = \sqrt{-1}$ is the imaginary unit and $\beta_k = \frac{2\pi K}{\lambda_z}$ is the wave number in the spanwise direction. λ_z is the spanwise wavelength of the fundamental Fourier mode. Also, the variables of physical space are represented by lowercase letters (f) and the variables of the Fourier space by capital letters (F).

After some calculations, the vorticity transport and the Poisson equations can be rewritten, for each k Fourier mode as

$$\frac{\partial \Omega_{x_k}}{\partial t} + \frac{\partial A_k}{\partial y} + i\beta_k B_k = \frac{1}{Re}\nabla_k^2 \Omega_{x_k} - i\beta_k F_{y_k} - \frac{\partial F_{z_k}}{\partial y}, \tag{22}$$

$$\frac{\partial \Omega_{y_k}}{\partial t} - i\beta_k C_k - \frac{\partial A_k}{\partial x} = \frac{1}{Re}\nabla_k^2 \Omega_{y_k} + \frac{\partial F_{z_k}}{\partial x} + i\beta_k F_{x_k}, \tag{23}$$

$$\frac{\partial \Omega_{z_k}}{\partial t} + \frac{\partial B_k}{\partial x} - \frac{\partial C_k}{\partial y} = \frac{1}{Re}\nabla_k^2 \Omega_{z_k} + \frac{\partial F_{x_k}}{\partial y} - \frac{\partial F_{y_k}}{\partial x}, \tag{24}$$

$$\frac{\partial^2 U_k}{\partial x^2} - \beta_k^2 U_k = i\beta_k \Omega_{y_k} - \frac{\partial^2 V_k}{\partial x \partial y}, \tag{25}$$

$$\frac{\partial^2 V_k}{\partial x^2} + \frac{\partial^2 V_k}{\partial y^2} - \beta_k^2 V_k = -\frac{\partial \Omega_{z_k}}{\partial x} - i\beta_k \Omega_{x_k}, \tag{26}$$

$$\frac{\partial^2 W_k}{\partial x^2} - \beta_k^2 W_k = \frac{\partial \Omega_{y_k}}{\partial x} + i\beta_k \frac{\partial V_k}{\partial y}, \tag{27}$$

where $\nabla_k^2 = \left(\frac{\partial^2}{\partial x^2} + \frac{\partial^2}{\partial y^2} - \beta_k^2\right)$ is the modified Laplacian operator.

4. RESULTS

The purpose of this section is to evaluate the 3D high order code using the the RFG method for imposing turbulent initial boundary conditions. For this, three-dimensional LES simulations of a turbulent boundary layer on a flat plate were performed and the results were compared with numerical data from the DNS simulations of Spalart (1988) (at $Re_\theta = 1410$) and LES simulations of Lund *et al.* (1998) (at $Re_\theta = 1530$). It is worth mentioning that Re_θ is calculated based on the momentum thickness.

The domain is discretized using 537 points and 335 points in the x- and y- direction respectively, with 32 Fourier modes in the transversal direction. The streamwise stepsize is $dx = 5 \times 10^{-3}$. The first wall-normal stepsize is $dy_0 = 1 \times 10^{-4}$ and the stretching factor is 1%. $dt = 10^{-4}$. Also, the velocity reference, viscosity and characteristic plate length are $U_\infty = 26 m/s$, $\nu = 1.55 \times 10^{-5} m^2/s$ and $L = 0.1m$, respectively. This combination of parameters ensures Re_θ between 400 and 1500 could be reached without being too close to inflow or the outflow. A thousand Fourier modes were adopted for the RFG method simulation ($N = 1000$). The time-scale of turbulence is $\tau = 10^{-2}$.

The mean velocity in streamwise direction is shown in Fig. 2, where the $Re_\theta = 989$ and $Re_\theta = 1123$, together with the mean profiles of Spalart (1988) and Lund *et al.* (1998). From this figure, it can be seen good agreement with the literature in the viscous sublayer ($y^+ < 5$, where y^+ is non-dimensional wall distance). On the order hand the streamwise mean velocity profile is overpredicted in the laminar-turbulent sublayer ($5 \le y^+ \le 70$) and in the turbulent sublayer ($y^+ > 70$). In general, the results for $Re_\theta = 1123$ are slightly better than for $Re_\theta = 989$.

The time and spanwise-averaged Reynolds stresses can be seen in Fig. 3, where also $Re_\theta = 989$ and $Re_\theta = 1123$. As can be noted, the $u'u'$ e $w'w'$ are also overpredicted, with a perceptible peak close to the wall. The $v'v'$ profile shows a good match with the literature.

Figure 4 shows the turbulence evolution by zxy isocontour crosscuts of the velocity components at different streawise positions. The evolution of the turbulence structures can be seen in all pictures.

5. CONCLUSIONS

This paper presented 3D LES simulations of a flat plate turbulent boundary layer to investigate a high order code in combination with the RFG technique for generating artificial turbulent initial boundary conditions. The numerical results were compared with numerical data from the DNS simulations of Spalart (1988) and LES simulations of Lund *et al.* (1998). In general, the numerical results showed good agreement with the literature, and the discrepancies found are being investigated.

6. ACKNOWLEDGEMENT

The author acknowledges the financial support received from FAPESP under 2011/00647-9 process.

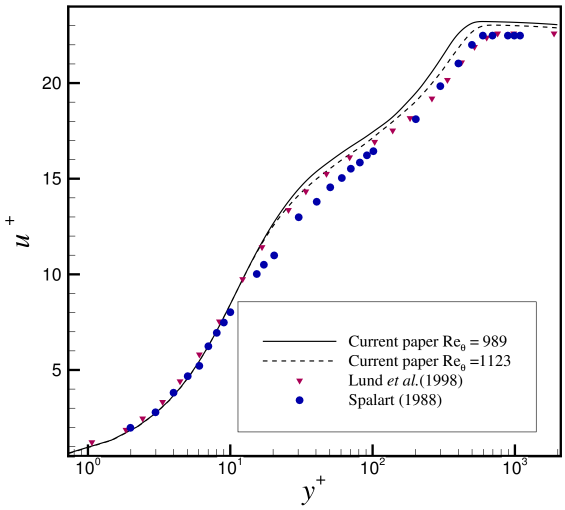

Figure 2. Mean velocity in streamwise direction u^+ as a function of y^+ (log scale) at $Re_\theta = 989$ and $Re_\theta = 1123$.

7. REFERENCES

Germano, M., Piomelli, U., Moin, P. and Cabot, W.H., 1991. "A dynamic subgridscale eddy viscosity model". *Physics of Fluids*, Vol. 4, pp. 1760–1765.

Jarrin, N., Prosser, R., Uribe, J.C., Benhamadouche, S. and Laurence, D., 2009. "Reconstruction of turbulent fluctuations for hybrid RANS/LES simulations using a Synthetic-Eddy Method". *International Journal of Heat and Fluid Flow*, Vol. 3, pp. 435–442.

Keating, A., Piomelli, U., Balaras, E. and Kaltenbach, H.J., 2004. "A priori and a posteriori tests of inflow conditions for large-eddy simulation". *Physics of Fluids*, Vol. 16, pp. 4696–4712.

Kraichnan, R.H., 1970. "Diffusion by a random velocity field". *Physics of Fluids*, Vol. 13, pp. 22–31.

Lesieur, M. and Métais, O., 1996. "New trends in Large-Eddy Simulations of turbulence". *Annual Review Fluid Mechanics*, Vol. 28, pp. 45–82.

Li, N., Balaras, E. and Piomelli, U., 2000. "Inflow conditions for Large-Eddy Simulations of mixing layers". *Physics of Fluids*, Vol. 12, pp. 935–938.

Lund, T., 1998. "Generation of turbulent inflow data for spatially-developing boundary layer simulations". *Journal of Computational Physics*, Vol. 140, pp. 233–258.

Lund, T.S., Wu, X. and Squires, K.D., 1998. "Generation of turbulent inflow data for spatially-developing boundary layer simulations". *Journal of Computational Physics*, Vol. 140, pp. 233–258.

Nicoud, F. and Ducros, F., 1999. "Subgrid-scale stress modelling based on the square of the velocity gradient". *Flow, Turbulence and Combustion*, Vol. 62, pp. 183–200.

Pamies, M., Weiss, P.E., Garnier, E., Deck, S. and Sagaut, P., 2009. "Generation of synthetic turbulent inflow data for large eddy simulation of spatially evolving wall-bounded flows". *Physics of Fluids*, Vol. 21.

Pope, S., 2000. *Turbulent flows*. Cambridge University Press.

Sagaut, P., 2006. *Large eddy simulation for incompressible flows*. Springer Verlag.

Smirnov, A., Shi, S. and Celik, I., 2001. "Random flow generation technique for Large Eddy Simulations and particle-dynamics modeling". *Journal of Fluids Engineering*, Vol. 123, pp. 359–371.

Spalart, P.R., 1988. "Direct simulation of a turbulent boundary layer up to $re_\theta = 1410$". *Journal Fluids Mechanics*, Vol. 187, pp. 61–98.

Wilcox, D.C., 1994. *Turbulence modeling for CFD*. DCW Industries.

8. RESPONSIBILITY NOTICE

The authors are the only responsible for the printed material included in this paper.

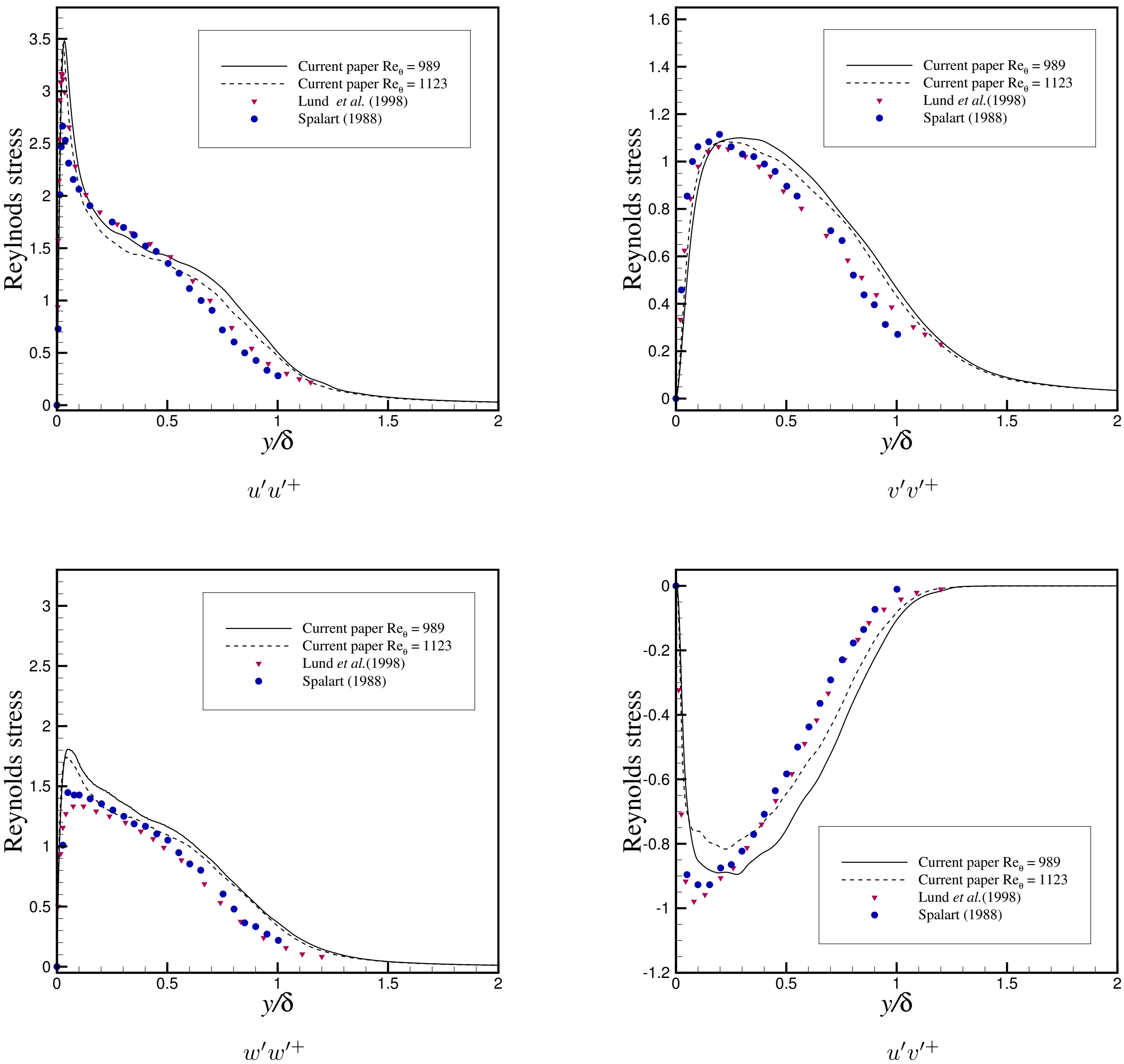

Figure 3. Reynolds stress as a function of $\frac{y}{\delta}$, where δ is the local turbulent boundary layer thickness. $Re_\theta = 989$ and $Re_\theta = 1123$.

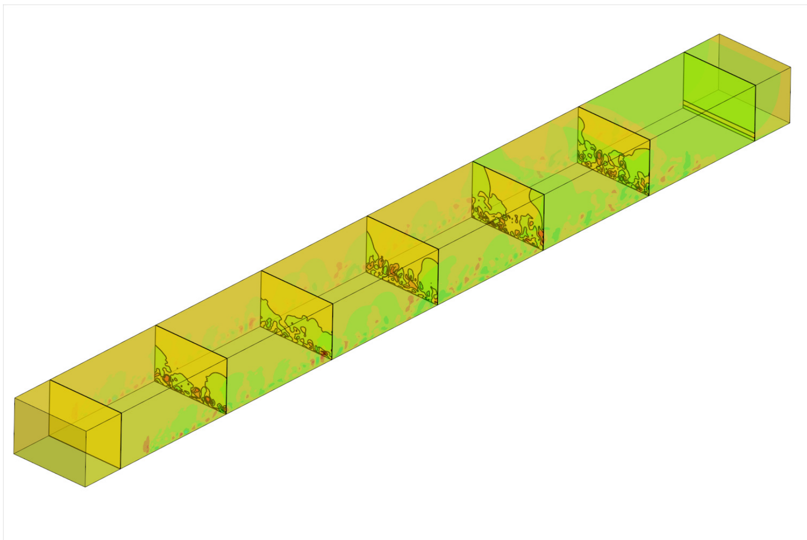

u velocity

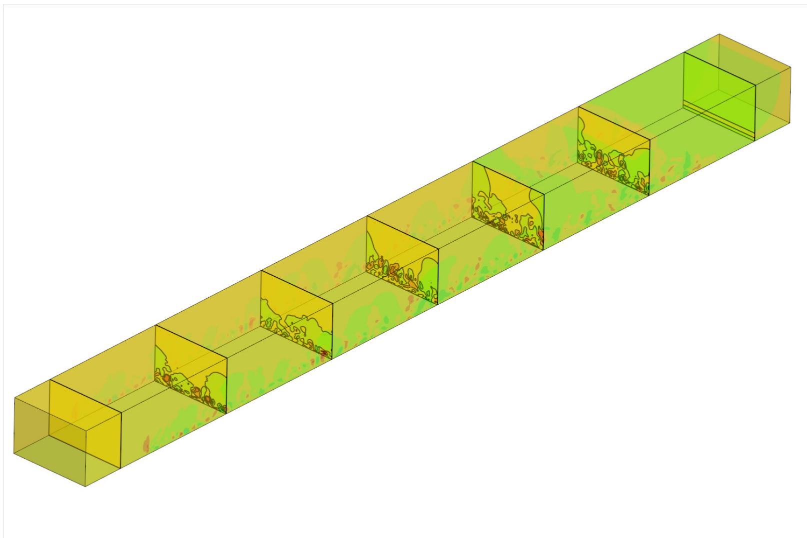

v velocity

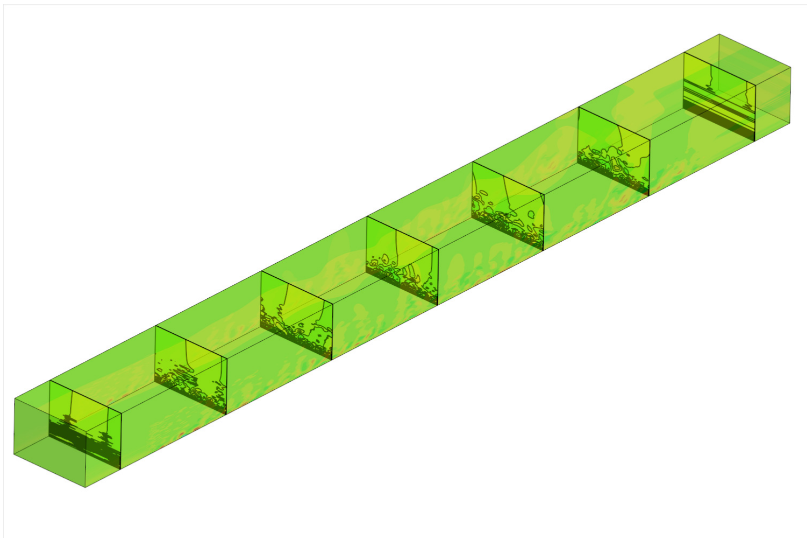

w velocity

Figure 4. Streamwise turbulence evolution.